HNPS Advances in Nuclear Physics

Vol 32 (2026)

HNPS2025

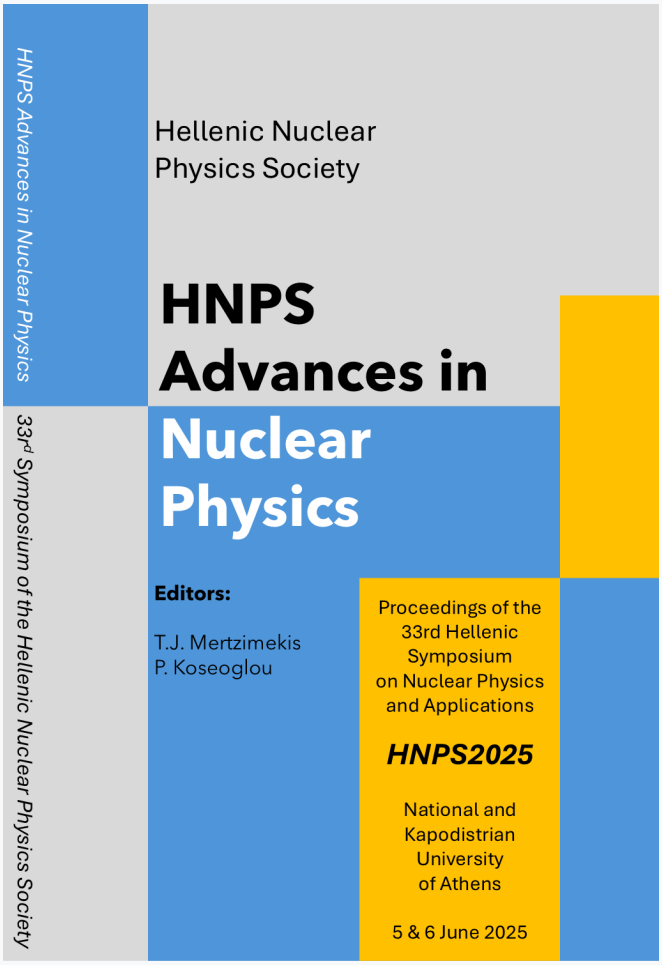

Analysis of historical events using sediment cores and nuclear methods: a case study at a deep basin at North Aegean Sea.

Anastasia Tasiopoulou, Christos Tsabaris, Effrosyni Androulakaki, Kyriaki Manta, Dionisis Patiris, Maria Diakaki

doi: 10.12681/hnpsanp.8837

To cite this article:

Tasiopoulou, A., Tsabaris, C., Androulakaki, E., Manta, K., Patiris, D., & Diakaki, M. (2026). Analysis of historical events using sediment cores and nuclear methods: a case study at a deep basin at North Aegean Sea. *HNPS Advances in Nuclear Physics*, *32*, 79–85. https://doi.org/10.12681/hnpsanp.8837

HNPS Advances in Nuclear Physics Vol. **32**, 79–85 (2025)
doi: 10.12681/hnpsanp.8837

Hellenic Nuclear Physics Society
Advances in Nuclear Physics
since 1990

ARTICLE

Analysis of historical events using sediment cores and nuclear methods: a case study at a deep basin at North Aegean Sea

A. Tasiopoulou,[*,1,2] C. Tsabaris,[1] E.G. Androulakaki,[1] K. Manta,[1] D.L. Patiris,[1] and M. Diakaki[2]

[1]Hellenic Centre for Marine Research, Institute of Oceanography, Anavyssos, Greece
[2]National Technical University of Athens, Department of Physics, Athens, Greece
*Corresponding author: atasiopoulou00@gmail.com

(Received: 07 Nov 2025; Accepted: 03 Dec 2025; Published: 04 Dec 2025)

Abstract
In this work, natural and artificial radioactivity levels were investigated in a sediment core collected from the Athos deep basin. The activity concentration was determined for the radionuclides ^{214}Pb, ^{210}Pb, and ^{214}Bi, ^{228}Ac, ^{208}Tl and ^{212}Pb, the natural radioisotope ^{40}K and the artificial radionuclide ^{137}Cs, using the gamma spectroscopy method. The sedimentation rate was estimated by applying radio-dating models, utilizing both the $^{210}Pb_{ex}$ method (CF:CS model) and the ^{137}Cs method, in order to validate the results. According to the $^{210}Pb_{ex}$ radiometric dating model, the sedimentation rate in the range of 0-8.25 cm is approximately (0.10±0.01) cm/y, while using the ^{137}Cs method, the sedimentation rate is (0.081±0.002) cm/y from the sampling period till the Chernobyl accident and (0.127±0.001) cm/y for the nuclear tests, respectively. The results suggest a relatively high sedimentation rate, with approximately 1 cm of sediment accumulating every 10 years. It appears that the sedimentation rate in this deep basin is influenced by multiple factors, due to land-sea interaction processes, as well as due to atmospheric fallout.

Keywords: HPGE; gamma-sprectrometry; radioactivity; sedimentation rate;

1. Introduction

Sediment cores refer to sediment samples collected from the seabed in large cylindrical tubes (more than 30 cm height). The core is separated in thin layers (~1 cm), each layer representing a distinct period in the past, which can be determined using radiodating methods. Sediment cores serve as valuable archives of environmental history, preserving physical, chemical and biological signals that reflect climate conditions, pollution levels and geological events. Techniques, such as excess ^{210}Pb dating and geochemical analysis, enable the reconstruction of temporal trends in sedimentation climate variability and anthropogenic footprints [1, 2]. These insights are essential for understanding long-term environmental processes and for supporting effective management strategies under

 ISBN 2654-007X (print), 2654-0088 (online).

changing global conditions.

This study aims to investigate sedimentation processes taking place in a deep basin near Athos, focusing on the accurate estimation of the sedimentation rate which will allow a reliable dating of the sediment layers. A sediment core was collected at a depth of 1180 m, using the box corer sampling method [3]. Gamma-ray spectrometry analyses were performed using a broad energy high-purity germanium (HPGe) detector at the Marine Environmental Radioactivity Laboratory of the Hellenic Centre for Marine Research (HCMR). The determination of the sedimentation rate in the selected core was carried out by applying radio-dating models using both the ^{210}Pb and the ^{137}Cs methods. The present study also involves the determination of the activity concentrations of the naturally occurring and anthropogenic radionuclides. During the samples preparation, the core was separated in fine intervals of 0.5 cm within the 0-15 cm depth range, to achieve better depth resolution in the upper layers, while at deeper layers the depth interval of the slices was increased to 1 cm. A total of 50 samples were collected and measured.

2. Materials and Methods

2.1 Study area

The sediment core of 44 cm length labeled as 'Marre-04' was collected with a box corer sampler from the Athos deep basin in the northern Aegean Sea. The sampling location (39°55.200'N, 24°19.200'E) corresponds to station 4, as shown in Fig. 1 depicting the wider study area.

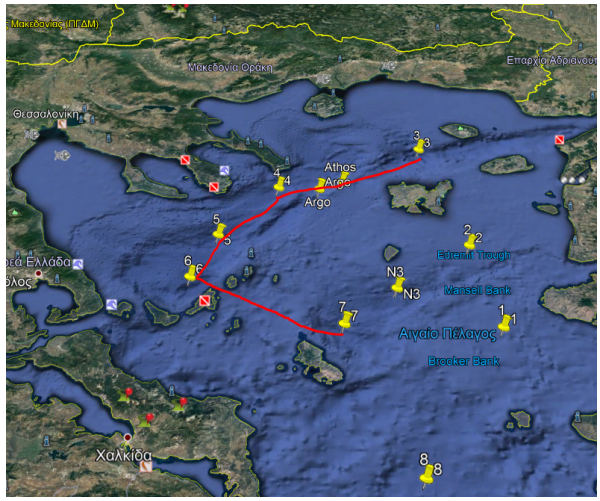

Figure 1. Map showing the location of the sampling site

The northern Aegean Sea constitutes a highly dynamic and complex oceanographic region of the Eastern Mediterranean. The inflow of cold and low-salinity Black Sea Water (BSW) through the Dardanelles Strait forms strong frontal zones with the warm and saline Levantine Surface Water (LSW). The mixing of these water masses, in combination with air-sea interactions, determines the general cyclonic circulation of the area and the vertical structure of the water column. The BSW is directed toward the Athos basin and the Samothraki shelf, contributing to the formation of intense frontal zones and complex hydrodynamic conditions [4, 5].

In Fig. 2, yellow arrows indicate the routes of the cold and low-salinity BSW, red arrows represent the currents of the intermediate Levantine waters and orange arrows show the routes of the mixed BSW-LSW waters. The hydrography of the Northern Aegean exhibits strong seasonal and spatial

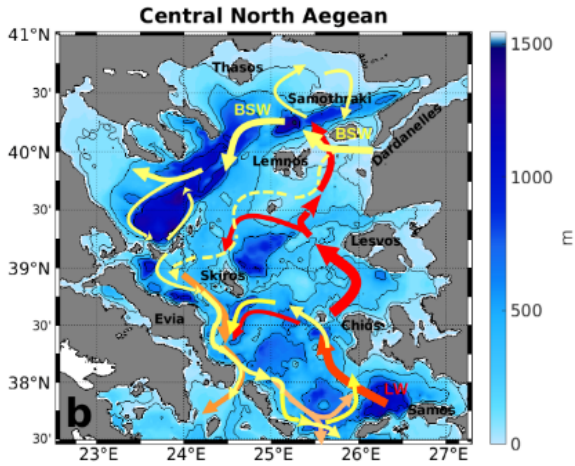

Figure 2. Schematic illustration of the surface and intermediate water t circulation [5]

variability, influenced by the intensity of the Black sea inflow, the atmospheric conditions and local processes. In the deeper layers, some of the densest waters of the entire Mediterranean are observed, making the northern Aegean an important region for dense water formation and an important area for oceanographic research [4, 5].

2.2 Preparation of samples

Sediment samples were prepared following the protocols [6] established by the International Atomic Energy Agency (IAEA). The 44 cm sediment core was sectioned at fine 0.5 cm intervals in the 15 cm depth range to achieve better depth resolution in the upper layers. From 15 to 30 cm depth, the core was sectioned at 1 cm intervals and at 2 cm from 30 cm to the core bottom. Each section was subsequently dried at 50°C in an oven. After drying, the samples were weighed and grounded using an agate mortar to ensure homogeneity. In total, 50 samples were obtained and then transferred into specialized cylindrical containers for further analysis. Two geometries were utilized (see Fig. 3): samples from the core section up to 30 cm depth were placed in small-geometry containers (36.22 mm diameter, 5.25 mm height), whereas samples from deeper layers were placed in large-geometry containers (68 mm diameter, 18 mm height) due to the increased sediment mass available at greater depths [7]. The final mass of each sample was then recorded. Each sample was hermetically sealed to achieve radioactive equilibrium.

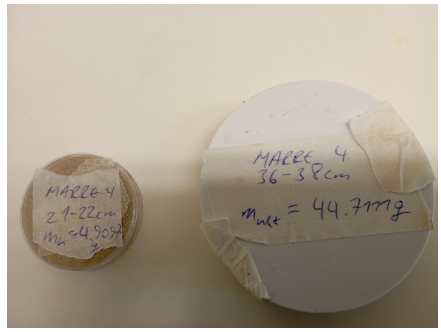

Figure 3. Cylindrical containers with powdered samples

2.3 Gamma-ray spectrometry

Gamma-ray spectroscopy analyses were performed using a broad energy High Purity Germanium (HPGe) detector (CANBERRA, BE5030). Each sample was measured over a 24 hours period. Samples were positioned in direct contact with the detector endcap to optimize the sample-to-crystal solid angle enhancing the detection efficiency. The same analysis was applied to the acquired background spectrum. For this measurement, an empty container was used with the same dimensions. This measurement was performed to account for the ambient background radiation and properly subtract it from the measurements on the sediment samples.

Experimental spectra were analyzed using the SPECTRW program [8]. The energy (E), photopeak resolution (FWHM), and full energy photopeak efficiency (FEPE) calibrations of the detector were performed (see Figs. 4, 5) using a standard reference source (IAEA soil, 36.22 mm diameter, 5.25 mm height) [7]. These parameters are fundamental properties of the detector and are critical for ensuring the reliability and accuracy of the experimental measurements. A separate reference source (68 mm diameter, 18 mm height) [7] was used for the calibrations to account for the samples collected from the deeper layers of the core. Subsequently, correction factors accounting for True Coincidence Summing (TCS) of simultaneously emitted gamma-rays and for sample self-absorption (ET), due to differences in density and composition between the reference sources and the samples, were calculated for each energy peak using EFFTRAN 4.5 software [9]. The photopeak efficiency at the specific energies FEPE was calculated using Eq. (1).

$$eff = \frac{cps}{m \cdot I_\gamma \cdot A} \cdot TCS \cdot ET \tag{1}$$

where (TCS , ET) are the correction factors; (A) is the activity of the reference sample, decay-corrected to the time of calibration; (m) is the mass (kg) of the sample and (I_γ) is the gamma-ray emission probability. The net count rate (cps), measured in counts/s, for each photopeak was derived from the spectra.

The activity concentration A (Bq/kg) for each radionuclide was estimated using the same equation, incorporating the full energy photopeak efficiencies (FEPE) previously calculated for each energy peak. The activity concentration measurements of the samples included naturally occurring radionuclides from the uranium and thorium decay chains (^{214}Pb, ^{214}Bi, ^{210}Pb for ^{238}U; ^{228}Ac, ^{208}Tl, ^{212}Pb for ^{232}Th), as well as ^{40}K and the artificial radionuclide ^{137}Cs.

2.4 Dating model

The natural radionuclide ^{210}Pb is widely used to date recent sediments (up to approximately 100 years). Its excess component $^{210}Pb_{ex}$ mainly originates from natural processes, such as floods and seismic events, which add sediment to the study area, as well as from atmospheric deposition of ^{222}Rn decay products attached to aerosols [1]. The exponential decrease of $^{210}Pb_{ex}$ activity with depth reflects sediment accumulation, providing the basis for estimating sedimentation rates and constructing age-depth models. In this study, the CF:CS model was applied, assuming a constant sediment flux and sedimentation rate [2]. The constant flux represents the steady input of excess ^{210}Pb to the sediment surface [1]. The activity concentration of $^{210}Pb_{ex}$ was determined as the difference between the total ^{210}Pb activity and that of ^{214}Pb ($^{210}Pb_{ex}$ = ^{210}Pb - ^{214}Pb).

3. Results and Discussion

3.1 Experimental calibration

The following calibrations of the detector were performed: energy (E), photopeak resolution (FWHM) and full energy photopeak efficiency (FEPE). In the analysis procedure, each activity concentration

was calculated using the experimental efficiency value for the relevant energies.

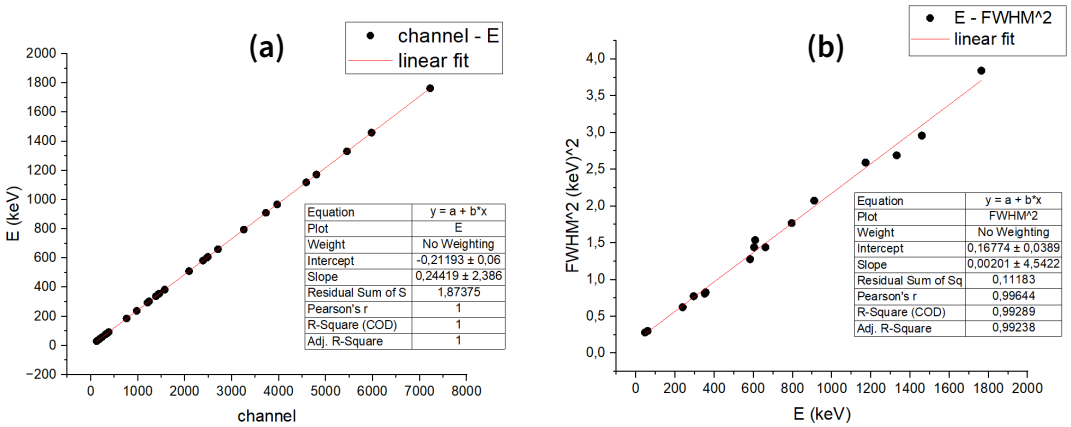

Figure 4. Calibration curves of (a) energy using $E_\gamma = a + b \cdot \text{channel}$, where $a = (-0.212 \pm 0.067)$ keV and $b = (0.24419 \pm 0.00002)$ keV/channel and (b) resolution using $\text{FWHM}^2 = a + b \cdot E_\gamma$, with $a = (0.167 \pm 0.039)$ keV^2 and $b = (0.00201 \pm 0.00004)$ keV.

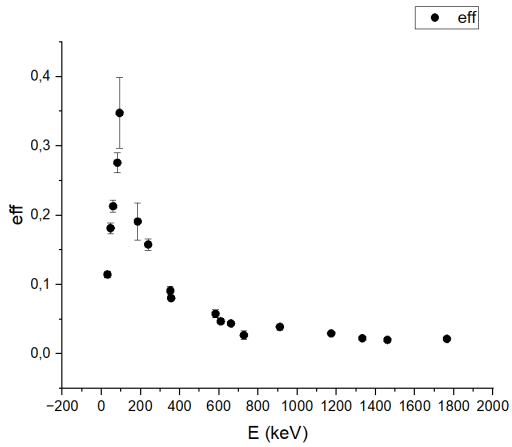

Figure 5. Calibration curve of absolute efficiency

3.2 Activity concentration results

The results of the activity concentration measurements are presented in Figs. 6, 7 and 8.

A clear Gaussian-type variation can be observed in both profiles within the 4-10 cm depth interval, likely related to a localized geological disturbance that influenced sediment accumulation. The activity concentrations of ^{214}Pb and ^{214}Bi are in very good agreement within uncertainties, as expected from the secular equilibrium of the ^{226}Ra decay series. Similarly, ^{228}Ac, ^{212}Pb, and ^{208}Tl show consistent values within uncertainties, as daughter products of the ^{232}Th decay chain. The agreement of the results among the different radionuclides of the same series confirms the reliability of the quantification method in the whole studied energy range.

The profiles of total ^{210}Pb and excess $^{210}\text{Pb}_{ex}$ exhibit similar distributions, with high activity concentrations near the surface (0-5 cm) that decrease exponentially with depth. For $^{210}\text{Pb}_{ex}$, this exponential decline reflects its radioactive decay over time. The clear exponential decrease indicates

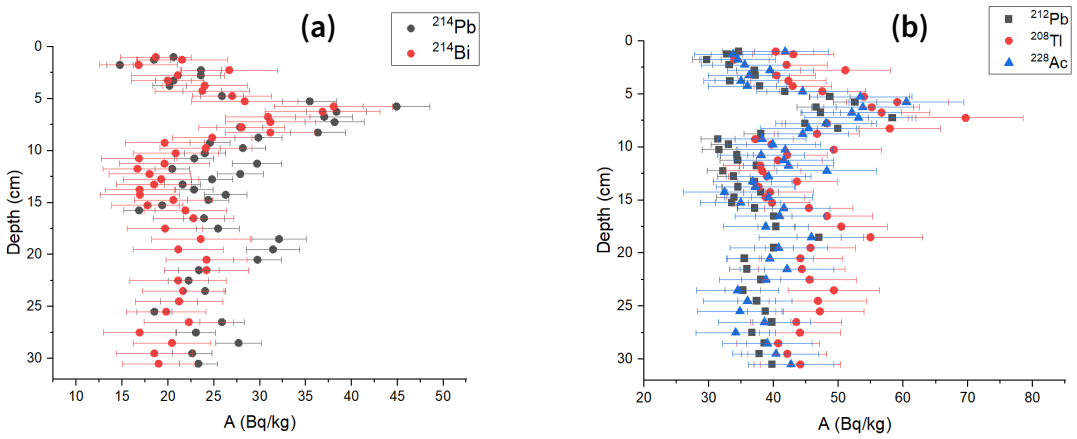

Figure 6. Activity concentration profiles of (a) uranium-series radionuclides and (b) thorium-series radionuclides as a function of core depth.

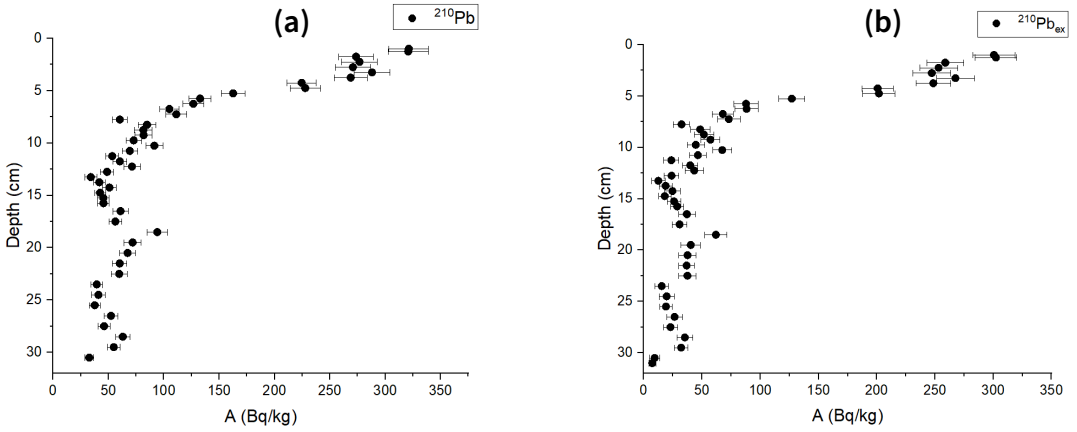

Figure 7. Activity concentration profiles of (a) ^{210}Pb (46 keV) and (b) $^{210}\mathrm{Pb}_{ex}$ as a function of core depth.

a constant sedimentation rate, which is a crucial factor for accurate radiometric dating. At depths greater than 30-35 cm, the activity concentrations reach low and nearly constant values.

The ^{40}K profile exhibits a nearly constant activity with depth, whereas in the ^{137}Cs profile, two distinct peaks are identified at depths of 2.75 cm and 7.25 cm, corresponding to the Chernobyl accident (1986) and the nuclear tests (1963), respectively.

From calculations using the CF:CS dating model, the sedimentation rate was determined to be (0.10±0.01) cm/y based on date from the upper 8.25 cm of the sediment core. Additionally, the sedimentation rate was estimated using the depth profile of ^{137}Cs activity concentrations. Based on the depths of the two peaks (2.75 cm and 7.25 cm) and considering the year of core collection (2020), the calculated sedimentation rates are $v_{Chernobyl}$=(0.081±0.002) cm/y and $v_{nuclear tests}$=(0.127±0.001) cm/y. The average sedimentation rate was v=(0.104±0.002) cm/y.

The two rates obtained from $^{210}\mathrm{Pb}_{ex}$ and ^{137}Cs dating methods are in very good agreement, confirming the reliability of the sediment dating results.

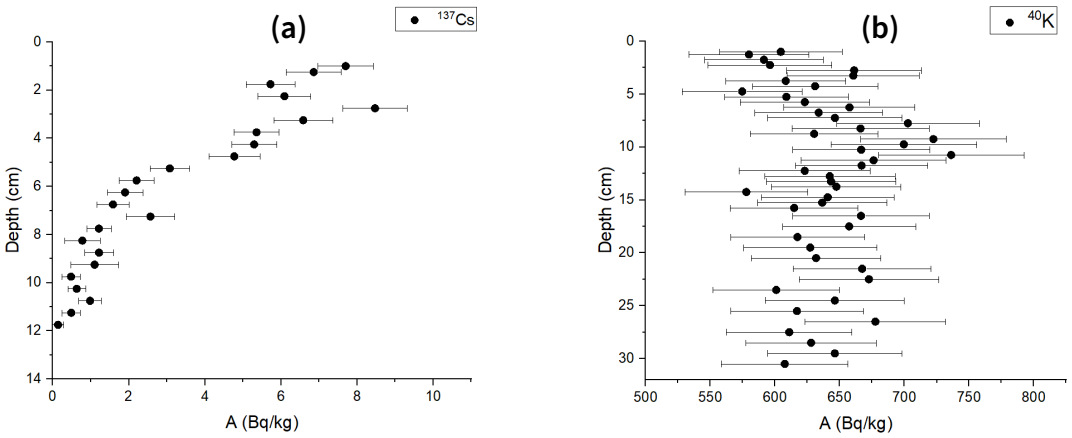

Figure 8. Activity concentration profiles of (a) ^{137}Cs (661 keV) and (b) ^{40}K (1460 keV) as a function of core depth.

4. Conclusion

The fine (0.5 cm) sectioning of the sediment core proved to be particularly effective in revealing additional information regarding the historical variability of chemical and physical magnitudes. More specifically, it enabled the clear identification of both the Chernobyl accident and the nuclear tests peaks in the ^{137}Cs vertical profile. This higher resolution led to more reliable results for the radiometric dating models. A clear Gaussian-type variation can also be observed in the natural radionuclide profiles (see Fig. 6), likely related to a localized geological disturbance that influenced sediment accumulation. This disturbance could be attributed to a possible seismic or flooding event that resulted in the deposition of additional sediment material. Moreover, the results suggest a relatively high sedimentation rate, with approximately 1 cm of sediment accumulating every 10 years. The sedimentation dynamics in this deep basin appear to be influenced by multiple factors, including land-sea interaction processes and atmospheric fallout.

Acknowledgements

The authors thank Dr. Kostas Kalfas for kindly providing the SPECTRW analysis program.

References

[1] A. Arias-Ortiz, P. Masqué, J. Garcia-Orellana, O. Serrano, I. Mazarrasa, N. Marba, C. Lovelock, P. Lavery, and C. Duarte. "Reviews and syntheses: 210Pb-derived sediment and carbon accumulation rates in vegetated coastal ecosystems – setting the record straight". In: *Biogeosciences* 15 (2018), pp. 6791–6818. DOI: 10.5194/bg-15-6791-2018.

[2] J.-A. Sanchez-Cabeza and A. Ruiz-Fernández. "210Pb sediment radiochronology: An integrated formulation and classification of dating models". In: *Geochim. Cosmochim. Acta* 82 (2012), 183–200. DOI: 10.1016/j.gca.2010.12.024.

[3] S. Blomqvist, N. Ekeroth, R. Elmgren, and P Hall. "Long overdue improvement of box corer sampling". In: *Mar. Eco. Prog. Ser.* 538 (2015), pp. 13–21. DOI: 10.3354/meps11405.

[4] V. Zervakis and D. Georgopoulos. "Hydrology and circulation in the North Aegean (eastern Mediterranean) throughout 1997-1998". In: *Medit. Mar. Sci* 3 (2002), pp. 5–19. DOI: 10.12681/mms.254.

[5] M. Potiris, I. Mamoutos, E. Tragou, V. Zervakis, D. Kassis, and D. Ballas. "Dense Water Formation in the North–Central Aegean Sea during Winter 2021–2022". In: *J. Mar. Sci. Eng.* 12 (2024), p. 221. DOI: 10.3390/jmse12020221.

[6] V. Kashparov G. Kis-Benedek G. Matisoff Yu. Onda N. Sanzharova S. Tarjan A. Tyler B. Varga U. Barnekow S. Fesenko. *Guidelines on Soil and Vegetation Sampling for Radiological Monitoring, Technical Reports Series No. 486.* Tech. rep. IAEA, 2019.

[7] G. Eleftheriou, C. Tsabaris, E.G. Androulakaki, F.K. Pappa, and D. Patiris. "High resolution gamma-ray spectrometry for routine measurements of environmental samples". In: *App. Rad. Isot.* 206 (2024), p. 111234. DOI: 10.1016/j.apradiso.2024.111234.

[8] C.A. Kalfas, M. Axiotis, and C. Tsabaris. "SPECTRW: A software package for nuclear and atomic spectroscopy". In: *Nucl. Instrum. Meth. Phys. Res. A* 830 (2016), pp. 265–274. DOI: 10.1016/j.nima.2016.05.098.

[9] Tim Vidmar. "EFFTRAN—A Monte Carlo efficiency transfer code for gamma-ray spectrometry". In: *NNucl. Instrum. Meth. Phys. Res. A* 550 (2005), pp. 603–608. ISSN: 0168-9002. DOI: 10.1016/j.nima.2005.05.055.